

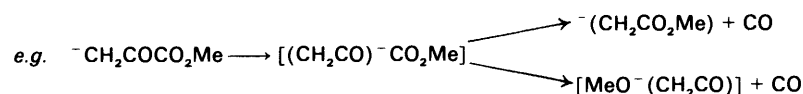
Anionic Rearrangement in the Gas Phase. The Collision-induced Loss of Carbon Monoxide from Deprotonated Pyruvates and Hydroxyacetates

Peter C. H. Eichinger,^a Roger N. Hayes,^b and John H. Bowie^{a,*}

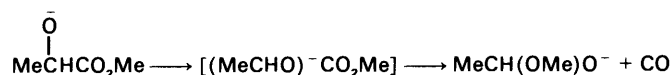
^a Department of Organic Chemistry, The University of Adelaide, South Australia 5001

^b Department of Chemistry, University of Nebraska-Lincoln, Lincoln, NE, 58588-0362, USA

Deprotonated pyruvates and hydroxyacetates, upon collisional activation, undergo loss of CO by anionic rearrangement through alkoxy-carbonyl ion complexes,

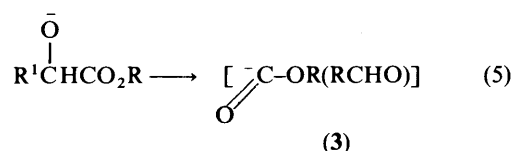
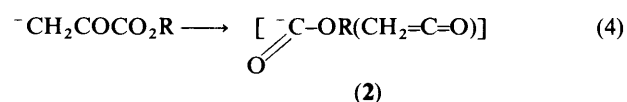
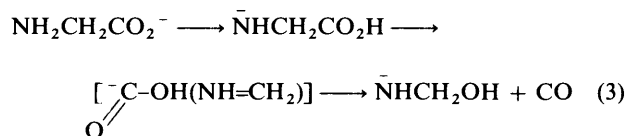
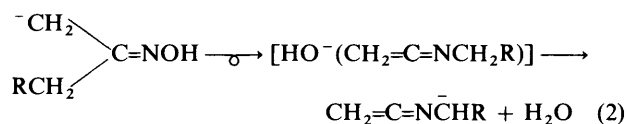
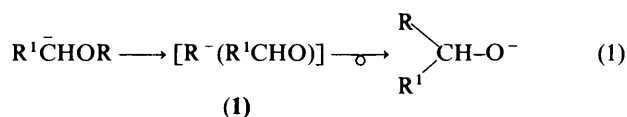


and



Such processes have been substantiated by labelling (²H, ¹³C), and product-ion studies.

Even-electron negative ions often undergo collision-induced rearrangement reactions in the gas phase when simple cleavage reactions are energetically unfavourable.¹ Recently, there have been reports of these species undergoing anionic 1,2-rearrangements, reactions which are thought to proceed through the intermediacy of ion-molecule complexes. For example, (i) the gas-phase Wittig rearrangement [equation (1)] proceeds through the anion complex (1) or the radical/radical anion intermediate [R[•](R¹CHO^{•-})],² and (ii) deprotonated oximes eliminate water perhaps *via* a negative-ion Beckmann rearrangement [equation (2)].³ Simple amino acids are also considered to undergo major fragmentation *via* a formal 1,2-anionic rearrangement: for example the base peak in the mass spectrum of deprotonated glycine is produced by loss of CO; a rationale for this process is shown in equation (3);⁴ here, the hydroxycarbonyl anion is a hydroxy-anion donor.⁵



It seems likely, from the amino acid analogy, that deprotonated pyruvates [equation (4)] and hydroxyacetates [equation (5)] should suffer loss of carbon monoxide through ion complexes (2) and (3), respectively. This paper thus seeks to answer two questions, *viz.* (i) what are the fragmentations of deprotonated pyruvates and hydroxyacetates, and (ii) if carbon monoxide is

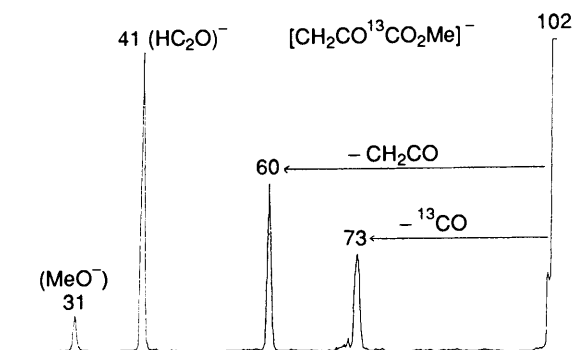


Figure 1. CA mass spectrum of $^-\text{CH}_2\text{CO}^{13}\text{CO}_2\text{Me}$. VG ZAB 2HF spectrometer. Electric sector scan. For details see Experimental section. A voltage of 1 000 V applied to the collision cell gave results which indicated that decomposition processes may occur both inside and outside the collision cell. A peak shifted from the normal value indicated a collision-induced process occurring in the collision cell, whereas an unshifted peak resulted from processes occurring outside the collision cell. The unshifted peak may be produced from a combination of unimolecular and collision-induced processes: the collision-induced component being due to leakage of collision gas from the cell. Results are [m/z (shifted component):unshifted component] 73(20:80), 60(70:30), 41(50:50), and 31(90:10).

Table 1. Collisional activation (CA) mass spectra of deprotonated alkyl pyruvates (${}^{-}\text{CH}_2\text{COCO}_2\text{R}$).^a

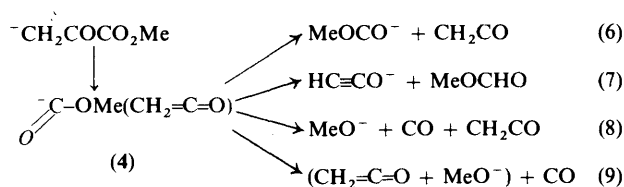
Precursor ion	Loss						Formation			
	H [•]	CO	¹³ CO	CH ₂ CO	(R - H)	(R - D)	RO ⁻	HC ₂ O ⁻	C ₃ H ₅ O ⁻	C ₃ D ₅ O ⁻
${}^{-}\text{CH}_2\text{COCO}_2\text{Me}$	25	45		58			14	100		
${}^{-}\text{CH}_2\text{CO}^{13}\text{CO}_2\text{Me}$	25		36	56			13	100		
${}^{-}\text{CH}_2\text{COCO}_2\text{Et}$	30	38 ^b		64	38 ^b		72	100		
${}^{-}\text{CH}_2\text{COCO}_2\text{CH}_2\text{CD}_3$	26	11		60		28	78	100		
${}^{-}\text{CH}_2\text{COCO}_2\text{C}_2\text{D}_5$	20	8				18	75	100		
${}^{-}\text{CH}_2\text{COCO}_2\text{Pr}^i$	85	7		100 ^c	100 ^c		87	47		
${}^{-}\text{CH}_2\text{COCO}_2\text{Bu}^i$		3		4	85		100	10	12	
${}^{-}\text{CH}_2\text{COCO}_2\text{C}(\text{CD}_3)_3$		2		5		70	100	8		8

^a Peak heights listed as relative abundance with respect to base peak (100%). ^b Composite peak, sharp Gaussian peak superimposed on dish-shaped peak. ^c Composite peak, sharp Gaussian peak superimposed on dish-shaped peak—Gaussian:dish *ca.* 100:45.

Table 2. Collisional activation (CA) and charge-reversal (CR) mass spectra of product ions in the mass spectra of deprotonated alkyl pyruvates.

Precursor ion (<i>m/z</i>)	Product ion (<i>m/z</i>)	Spectrum type	Spectrum [<i>m/z</i> (abundance)]
${}^{-}\text{CH}_2\text{COCO}_2\text{Me}$ (101)	MeOCO ⁻ (59)	CA MS/MS/MS CR MS/MS/MS	31 (100) 44 (16), 30 (22), 29 (100), 28 (61), 15 (30)
${}^{-}\text{CH}_2\text{COCO}_2\text{Me}$ (101)	${}^{-}(\text{CH}_2\text{CO}_2\text{Me})$ (73)	CA MS/MS ^{a,b} CA MS/MS ^{a,b}	58 (7), 41 (100), 31 (2) 59 (7), 57 (2), 45 (8), 44 (12), 42 (100), 31 (6), 29 (29), 27 (13), 15 (18), 14 (7), 13 (3)
${}^{-}\text{CH}_2\text{COCO}_2\text{Me}$ (101)	(101 - CO) (73)	CA MS/MS/MS ^{c,d} CR MS/MS/MS ^{c,d}	41 (100) 42 (60), 41 (100), 31 (45), 29 (30), 27 (11), 15 (17), 14 (10)
${}^{-}\text{CH}_2\text{COCO}_2\text{Bu}^i$ (143)	${}^{-}(\text{CH}_2\text{COMe})$ (57)	CA MS/MS/MS ^{c,e} CR MS/MS/MS ^{c,e}	56 (100), 41 (60) 55 (10), 43 (65), 42 (100), 41 (25), 39 (60), 29 (40), 27 (40), 26 (15), 15 (15)

^a Decomposition data for *m/z* 73 formed in the ion source. ^b MS/MS data for authentic ${}^{-}(\text{CH}_2\text{CO}_2\text{Me})$ (formed by deprotonation of MeCO₂Me) are: (CA) 58 (7), 41 (100), and 31 (4); (CR) 59 (8), 57 (2), 45 (10), 44 (10), 42 (100), 31 (6), 29 (30), 27 (15), 15 (17), 14 (8), and 13 (3). ^c Weak spectra: time average of 100 scans. Peaks < 10% of base peak are lost in background noise. ^d The ion formed in the source is *exclusively* ${}^{-}(\text{CH}_2\text{CO}_2\text{Me})$, but that formed in the collision cell is clearly a mixture of ${}^{-}(\text{CH}_2\text{CO}_2\text{Me})$ and [MeO⁻(CH₂CO)]. The presence of the latter ion (the ion-molecule complex) is indicated by the *additional* peaks in the CR spectrum at *m/z* 31 (CH₃O⁺) and 41 (HC₂O⁺). ^e The spectra are characteristic of ${}^{-}(\text{CH}_2\text{COMe})$ (*cf.* ref. 13).

**Scheme 1.**

lost from the various parent ions, what are the structures of the product ions so formed?

A. The Fragmentations of Deprotonated Pyruvates.—Collisional activation mass spectra (MS/MS) are listed in Table 1

* The process $\text{MeOCO}^{-} \longrightarrow \text{MeO}^{-} + \text{CO}$ is thermoneutral [ΔH° , CO⁷ and MeO⁻⁸ are -110 and -139 kJ mol⁻¹, respectively; MeOCO⁻ -249 kJ mol⁻¹ (calculated from reported data in refs. 7, 9, and 10)].

† A reviewer has suggested that the reactions of MeOCO⁻ may be interpreted in terms of a structure [MeO⁻(CO)]. Calculations¹¹ tend to favour the structure MeOCO⁻.

‡ The species *m/z* 73 is also formed in the ion source of the mass spectrometer. In this case the data in Table 2 show the ion to correspond *exclusively* to ${}^{-}(\text{CH}_2\text{CO}_2\text{Me})$. Thus for source decompositions, equation (9) yields solely the 1,2 rearrangement product.

and particular examples are illustrated in Figures 1 and 2. Collisional activation and charge reversal⁶ (positive-ion) mass spectra (MS/MS/MS) of certain product ions are recorded in Table 2. Fragmentations are shown for the prototypical example of methyl pyruvate in Figure 1 and Scheme 1.

All of the major fragmentations shown in Figure 1 may be rationalised as reactions of methoxycarbonyl complex (4). In this context, the mass spectrum of MeOCO⁻ [*m/z* 59, *cf.* MeO¹³CO⁻ (*m/z* 60) in Figure 1] is shown in Table 2; it exhibits only fragmentation to MeO⁻.^{*} Thus the methoxycarbonyl complex (4) may liberate MeOCO⁻ [equation (6)], MeOCO⁻ may act as a base [equation (7)], it may liberate MeO⁻ [equation (8)], or it may donate MeO⁻ to the neutral ketene with subsequent elimination of carbon monoxide.† Figure 1 shows loss of ¹³CO, and the product ion, *m/z* 73, is identified as a mixture of ${}^{-}(\text{CH}_2\text{CO}_2\text{Me})$ and [MeO⁻(CH₂CO)] by the various spectra listed in Table 2.‡

As the alkyl group of the deprotonated alkyl pyruvate increases in size, two changes are particularly noticeable; *viz.* (i) the loss of carbon monoxide decreases markedly in comparison with other processes, and (ii) the elimination of an alkene from the alkyl chain (for R ≥ Et) becomes more pronounced. The latter reaction is an internal elimination reaction of the type observed previously for enolates,¹² amides,¹³ and unsaturated ethers.¹⁴ It is best illustrated by reference to Figure 2 where the loss of CD₂CD₂ gives rise to the dish-shaped peak centred on *m/z* 88. Dish-shaped peaks resulting from such processes (see also Table 1) are characteristic of reactions with substantial

Table 3. Collisional activation (CA) mass spectra of deprotonated α -hydroxy esters and RCHCO_2Me ions

Precursor ion	Loss						Formation		
	Me^\cdot	CO	^{13}CO	MeOH	HCO_2Me	$\text{H}^{13}\text{CO}_2\text{Me}$	MeOCO^-	$\text{MeO}^{13}\text{CO}^-$	MeO^-
$[\text{MeCH}(\text{OH})\text{CO}_2\text{Me} - \text{H}]^-$	15	100		4	20		7		2
$[\text{MeCH}(\text{OH})^{13}\text{CO}_2\text{Me} - \text{H}]^-$	13		100	3		12		4	2
$[\text{EtCH}(\text{OH})\text{CO}_2\text{Me} - \text{H}]^-$	4	100		2	39		3		2
$[\text{Pr}^i\text{CH}(\text{OH})\text{CO}_2\text{Me} - \text{H}]^-$	4	100		2	54		2		1
$[\text{Bu}^i\text{CH}(\text{OH})\text{CO}_2\text{Me} - \text{H}]^-$	2	100		1			1		1
$[\text{PhCH}(\text{OH})\text{CO}_2\text{Me} - \text{H}]^-$	10	100		52	8		0.5		
$\text{PhCH}(\text{O}^-)\text{CO}_2\text{Me}^b$		100		4 ^c	3		0.3		

^a Peak height—listed as relative abundances with respect to base peak (100%). ^b Prepared by the $\text{S}_{\text{N}}2(\text{Si})$ reaction shown in equation (12). ^c The minor loss of MeOH was not expected. A 1,2 H^- shift forming $\text{PhC}(\text{OH})\text{CO}_2\text{Me}$ {which could then lose MeOH [equation (15)]} seems unlikely, because of the high activation energy of such a process. Perhaps cyclisation forms the ion pair $[(\text{PhCH} - \text{C}=\text{O})\text{MeO}^-]$ which eliminates MeOH in this instance

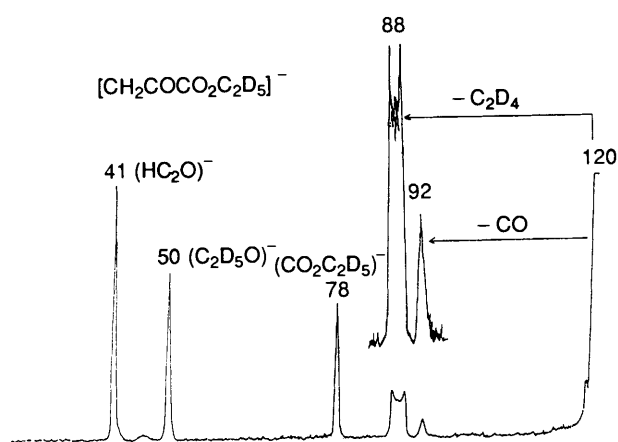
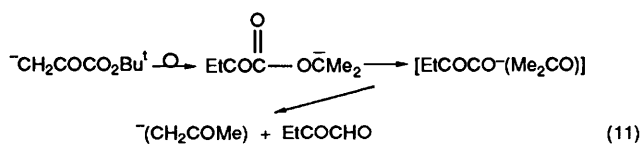
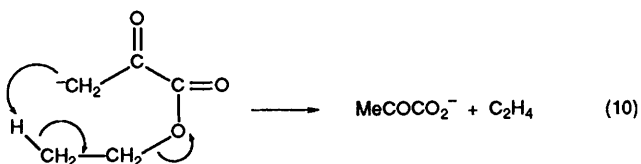


Figure 2. CA mass spectrum of $[\text{CH}_2\text{COCO}_2\text{CD}_2\text{CD}_3]^-$, VG ZAB 2HF spectrometer. Electric sector scan. Width of m/z 88 at half-height = 151 ± 2 V.

reverse activation energies.¹² In this case the elimination reaction must proceed through a seven-centre state [equation (10)]; most reported examples have proceeded through six-centre transition states.^{12,13}



Finally the *t*-butyl derivative yields an ion of empirical formula $\text{C}_3\text{H}_5\text{O}^-$, a species not observed in the other spectra (Table 1). The analogous peak in the spectrum (Table 1) of the D_9 derivative corresponds to $\text{C}_3\text{D}_5\text{O}^-$. The product ion is identified as $^-(\text{CH}_2\text{COMe})$ by its MS/MS/MS data (Table 2); its formation must therefore be preceded by methyl migration

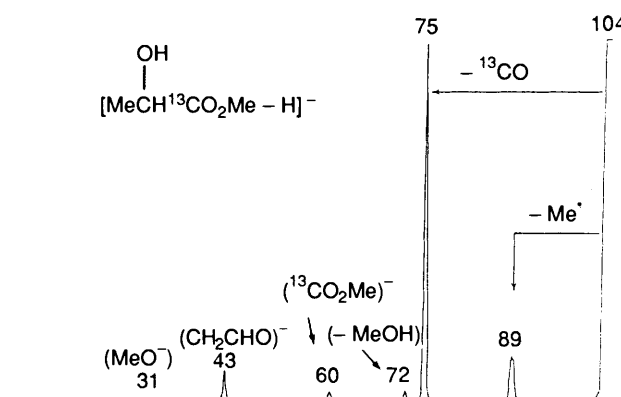


Figure 3. CA mass spectrum of $[\text{MeCH}(\text{OH})^{13}\text{CO}_2\text{Me} - \text{H}]^-$, VG ZAB 2HF spectrometer. Electric sector scan. A voltage of 1 000 V applied to the collision cell gave the following results: [m/z (shifted component: unshifted component)] see legend to Figure 1 for explanation] 89 (50:50), 75 (35:65), 72 (70:30), 60 (90:10), 43 (80:20), and 31 (80:20).

from the *t*-butyl group to either carbon or oxygen. The example of migration to carbon is shown in equation (11).

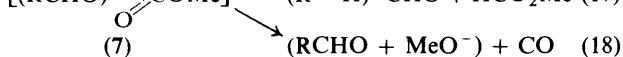
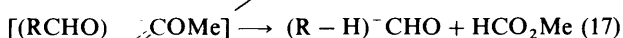
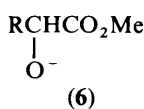
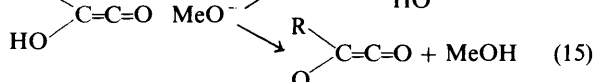
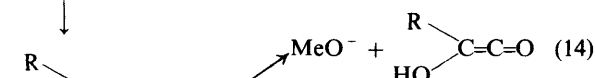
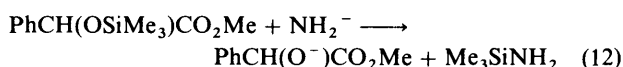
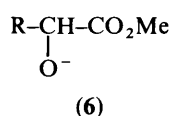
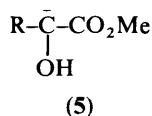
B. The Fragmentations of Deprotonated α -Hydroxy Esters.—Mass spectra of α -hydroxy methyl esters are listed in Table 3: a particular example is illustrated in Figure 3. MS/MS/MS data of selected product ions are collected in Table 4. The reaction between NH_2^- and α -hydroxy esters forms two deprotonated species, (5) and (6), and the resulting mass spectra (Table 3 and Figure 3) show fragmentations of both ions. We have synthesized a particular alkoxide ion specifically by the $\text{S}_{\text{N}}2(\text{Si})$ reaction shown in equation (12): its mass spectrum is listed in Table 3. The fragmentations of species (5) and (6) are illustrated in Figure 3. Fragmentations of the enolate ion (5) are minor, and follow well established routes,¹² *viz.*, radical cleavage to give a stabilised radical anion [equation (13)] and formation of an ion-molecule complex which undergoes both direct cleavage [equation (14)] and proton transfer between the components of the ion-molecule complex [equation (15)]. Major fragmentation proceeds through the alkoxide (6): all reactions can be rationalised by the intermediacy of ion-molecule complex (7) which would undergo direct displacement [equation (16)], internal deprotonation [equation (17)], and decarbonylation [equation (18)].

The decarbonylation reaction [equation (18)] produces the

Table 4. Collisional activation (CA) and charge-reversal (CR) MS/MS/MS data for product ions in the mass spectra of deprotonated α -hydroxy esters.

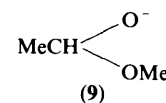
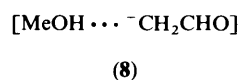
Precursor ion (m/z)	Product ion (m/z)	Spectrum type	Spectrum [m/z (abundance)]
$\begin{array}{c} \text{OH} \\ \\ (\text{MeCHCO}_2\text{Me} - \text{H})^- \\ (103) \end{array}$	$103 - \text{CO}^a \\ (75)$	CA CR	43 (100) 59 (3), 44 (33), 43 (100), 42 (68), 33 (15), 32 (30), 31 (89), 29 (55), 27 (29), 15 (56), 14 (9), 13 (2)
$\begin{array}{c} \text{OH} \\ \\ (\text{EtCHCO}_2\text{Me} - \text{H})^- \\ (117) \end{array}$	$117 - \text{CO} \\ (89)$	CA CR	57 (100) 58 (42), 57 (81), 56 (22), 41 (22), 39 (52), 33 (22), 31 (46), 29 (100), 27 (42), 15 (14), 14 (6)
$\begin{array}{c} \text{OH} \\ \\ (\text{Bu}^t\text{CHCO}_2\text{Me} - \text{H})^- \\ (145) \end{array}$	$145 - \text{CO} \\ (117)$	CA CR	101 (5), 87 (100), 85 (6), 31 (45) 101 (4), 86 (6), 85 (4), 71 (8), 69 (11), 58 (10), 57 (100), 55 (15), 43 (16), 41 (72), 39 (42), 31 (11), 29 (43), 27 (16)
$\begin{array}{c} \text{OH} \\ \\ (\text{PhCHCO}_2\text{Me} - \text{H})^- \\ (165) \end{array}$	$165 - \text{CO} \\ (137)$	CA CR	121 (5), 107 (100), 105 (76), 104 (12), 77 (16), 31 (14) 121 (10), 105 (100), 90 (6), 77 (82), 63 (6), 51 (22), 50 (18), 39 (6)

^a Authentic $\text{MeCH}(\text{OMe})\text{O}^-$ was made by the following $\text{S}_{\text{N}}2$ reaction in the ion source of the VG ZAB spectrometer: $\text{MeCH}(\text{OMe})_2 + \text{MeO}^- \longrightarrow \text{MeCH}(\text{OMe})\text{O}^- + \text{MeOMe}$. The MS/MS spectra of $\text{MeCH}(\text{OMe})\text{O}^-$ are: (CA) 43 (100); (CR) 59 (2), 44 (38), 43 (100), 42 (72), 33 (12), 32 (28), 31 (92), 29 (49), 27 (20), and 15 (10). Thus the spectra of $\text{MeCH}(\text{OMe})\text{O}^-$ and m/z 75 are very similar with the exception of the abundances of the low mass peaks in the CR spectra.



base peak in all spectra. But what is the structure of the product ion? Is it a proton-bound dimer or a tetrahedral species? The MS/MS/MS data in Table 4 assist with the determination of the product structure. In the cases of the Bu^t and Ph derivatives (Table 4), the adduct is likely to correspond to the tetrahedral species $\text{RCH}(\text{OMe})\text{O}^-$ since the carbon atom α to the carbonyl group bears no hydrogen, thus limiting the possibility of H-bonded adducts. The complex CA spectra of the appropriate adducts (Table 4) support this proposal. However, other cases are not so straightforward. In the simplest case, $[\text{MeCH}(\text{OH})-$

$\text{CO}_2\text{Me} - \text{H}]^-$ could form both species (8) and (9), and both possible product ions should fragment to yield MeO^- and $(\text{CH}_2\text{CHO})^-$. We have made species (9) by an independent route; its spectra (Table 4) are similar to those of the rearrangement ion. Thus the reaction shown in equation (18) yields mainly $\text{RCH}(\text{OMe})\text{O}^-$, and is formally a 1,2 anionic rearrangement.*



In conclusion, deprotonated pyruvates and α -hydroxyacetates decompose preferentially through hydroxycarbonyl anion complexes, a major fragmentation route of which is loss of carbon monoxide.

Experimental

MS/MS data were obtained with a VG ZAB 2HF mass spectrometer,[†] details of which have been given previously.¹² The specific conditions are: the collisional ionisation slit in the source, ion-source temperature 150 °C, electron energy 70 eV, and accelerating voltage 7 kV. Samples were introduced through the septum inlet which was maintained at 150 °C (the phenyl hydroxyacetate was introduced *via* the direct probe without heating). The source pressure of substrate was 5×10^{-7} Torr (1 Torr = 133.322 Pa). The deprotonating agent (and

* The experimental data shown in Table 4 do not exclude the possibility of the formation of a minor amount of the ion complex (8). A reviewer has suggested that we should also make species (8) and compare its spectrum with that of the rearrangement ion. We agree: unfortunately, there is no way we can make this ion exclusively and measure its spectra with the facilities available to us.

[†] VG Instruments, Wythenshawe, Manchester, M23 9LE, UK; model ZAB 2HF.

desilylating agent) was NH_2^- (from NH_3 , source pressure of NH_3 1×10^{-5} Torr). The estimated total source pressure was 10^{-1} Torr. Helium was used as the collision gas in the second collision cell. The measured pressure was 2×10^{-7} Torr, producing a 10% reduction in the main beam, and corresponding essentially to single-collision conditions. The electric sector scan mode was used. Peak widths at half-height are a mean of ten individual scans, and (in general), are correct to within ± 2 V. Charge-reversal (CR) spectra were obtained by collision-induced charge stripping of the negative ion to the corresponding decomposing positive ion.⁶

MS/MS/MS data were produced using an MS 50 TA instrument of which details have been reported.¹⁵ Neutral substrates were deprotonated by MeO^- (from MeONO^{16}) in a Kratos Mark IV chemical ionisation source: ion-source temperature 100 °C, electron energy 280 eV, emission current 500 μA , and accelerating voltage 8 kV. Samples were introduced through an all-glass heated inlet system at 100 °C. The indicated source pressure of substrate was 2×10^{-5} Torr and of methyl nitrite 1×10^{-6} Torr, giving an estimated source pressure of ca. 10^{-1} Torr. The indicated pressure of helium in the collision cells was 2×10^{-6} Torr, giving a decrease in the main beam signal of 30%.

The following compounds were prepared by reported methods: methyl,¹⁷ ethyl,¹⁸ isopropyl,¹⁹ and t-butyl pyruvates;¹⁷ methyl lactate,¹⁷ methyl 2-hydroxybutyrate,²⁰ methyl 2-hydroxy-3-methylbutyrate,²¹ methyl 2-hydroxy-3,3-dimethylbutyrate,²² methyl hydroxy(phenyl)acetate and methyl phenyl(trimethylsiloxy)acetate.²⁴

Labelled Compounds.—The deuterium-labelled compounds ethyl [2,2,2- $^2\text{H}_3$]-, ethyl [$^2\text{H}_5$]-, and t-butyl [$^2\text{H}_9$]-pyruvate were prepared using, respectively, [2,2,2- $^2\text{H}_3$]ethanol, [$^2\text{H}_5$]ethanol, and [$^2\text{H}_9$]-t-butyl alcohol, by the standard procedure.¹⁷ Incorporation: D_3 , D_5 , and D_9 99%.

Methyl [1- ^{13}C]Lactate.—A mixture of methanesulphonic acid (1.5 g) and anhydrous methanol (5 cm^3) was added to a suspension of sodium [1- ^{13}C]lactate (0.53 g)²⁵ in 1,2-dichloroethane (20 cm^3). The reaction mixture was heated under reflux for 24 h. The acid was neutralised with 0.1 mol dm^{-3} sodium methoxide in methanol, and distillation yielded methyl [1- ^{13}C]lactate (0.38 g, 77%), b.p. 145 °C/760 mmHg (^{13}C 91%).

Methyl [1- ^{13}C]pyruvate was prepared by a standard method²⁵ from methyl [1- ^{13}C]lactate (^{13}C 91%).

Acknowledgements

This work was supported by the Australian Research Council and the Midwest Center for Mass Spectrometry, an NSF Instrumental facility.

References

- 1 J. H. Bowie, *Mass Spectrom. Rev.*, 1990, **6**, 349.
- 2 P. C. H. Eichinger, J. H. Bowie, and T. Boumenthal, *J. Org. Chem.*, 1986, **51**, 5078; P. C. H. Eichinger and J. H. Bowie, *J. Chem. Soc., Perkin Trans. 2*, 1987, 1499; 1988, 497.
- 3 G. W. Adams, J. H. Bowie, and R. N. Hayes, *J. Chem. Soc., Perkin Trans. 2*, 1990, 1989, 2159.
- 4 M. Eckersley, J. H. Bowie, and R. N. Hayes, *Int. J. Mass Spectrom. Ion Processes*, 1989, **93**, 199.
- 5 J. C. Sheldon and J. H. Bowie, *J. Am. Chem. Soc.*, 1990, **112**, 2424.
- 6 J. H. Bowie and T. Blumenthal, *J. Am. Chem. Soc.*, 1975, **97**, 2951; J. E. Szulejko, J. H. Bowie, I. Howe, and J. H. Beynon, *Int. J. Mass Spectrom. Ion Phys.*, 1980, **13**, 76.
- 7 S. W. Benson, 'Thermochemical Kinetics,' Wiley-Interscience, New York, 1976.
- 8 P. C. Engelking, G. B. Ellison, and W. C. Lineberger, *J. Chem. Phys.*, 1978, **69**, 1826.
- 9 H. M. Rosenstock, K. Draxl, B. W. Steiner, and J. T. Herron, *J. Phys. Chem. Ref. Data*, 1977, **6**, Suppl. 1.
- 10 C. H. DePuy, J. J. Grabowski, V. M. Bierbaum, S. Ingemann, and N. M. M. Nibbering, *J. Am. Chem. Soc.*, 1985, **107**, 1093.
- 11 J. Chandrasekhar, J. G. Andrade, and P. v R. Schleyer, *J. Am. Chem. Soc.*, 1981, **103**, 5612.
- 12 M. B. Stringer, J. H. Bowie, and J. L. Holmes, *J. Am. Chem. Soc.*, 1986, **108**, 3888.
- 13 M. J. Raftery and J. H. Bowie, *Int. J. Mass Spectrom. Ion Processes*, 1988, **85**, 167.
- 14 R. J. Waugh, R. N. Hayes, P. C. H. Eichinger, K. M. Downard, and J. H. Bowie, *J. Am. Chem. Soc.*, 1990, **112**, 2537.
- 15 D. J. Burinsky, R. G. Cooks, E. K. Chess, and M. L. Gross, *Anal. Chem.*, 1982, **54**, 295; M. L. Gross, E. K. Chess, P. A. Lyon, F. W. Crow, S. Evans, and H. Tudge, *Int. J. Mass Spectrom. Ion Phys.*, 1982, **42**, 243.
- 16 D. P. Ridge and J. L. Beauchamp, *J. Am. Chem. Soc.*, 1974, **96**, 3595.
- 17 R. O. Clinton and S. C. Laskowski, *J. Am. Chem. Soc.*, 1948, **70**, 3136.
- 18 A. A. Goldberg and W. Kelly, *J. Chem. Soc.*, 1947, 1374.
- 19 A. Adkins, R. M. Eloffson, A. G. Rossow, and C. C. Robinson, *J. Am. Chem. Soc.*, 1949, **71**, 3624.
- 20 C. A. Bischoff and P. Walden, *Justus Liebigs Ann. Chem.*, 1894, **279**, 100; W. Reppe and V. Mitarbeitern, *ibid.*, 1955, **596**, 50, 69.
- 21 E. Schmidt and R. Sacktleben, *Justus Liebigs Ann. Chem.*, 1878, **193**, 106; Y. Izumi, M. Imaida, H. Fukawa, and S. Akabori, *Bull. Chem. Soc. Jpn.*, 1963, **36**, 21.
- 22 R. C. Fuson, H. Gray, and J. J. Gouza, *J. Am. Chem. Soc.*, 1939, **61**, 1937; A. Richard, *Ann. Chim. Phys.*, 1910, **21**, 398.
- 23 S. F. Acree, *Ber. Dtsch. Chem. Ges.*, 1904, **37**, 2767.
- 24 D. J. Costa, N. E. Boutin, and J. G. Riess, *Tetrahedron*, 1974, **30**, 3793.
- 25 W. Sakami, W. E. Evans, and S. Gurin, *J. Am. Chem. Soc.*, 1947, **69**, 1110.

Paper 0/01663B

Received 12th April 1990

Accepted 8th June 1990